PUBELESE PUBLISHER

JOAASR Journal of Advanced Applied Scientific Research

Biosynthesis of silver nanoparticles derived *Acorus calamus* rhizome extract and their biomedical application

B. Abirami[1], D.Siva[1], S.Abinaya[1], D.Praveenkumar[1], A.Vinothkumar[1], G.Saravanan[1] and S. Achiraman[1*]

[1] Dept .of Environmental Biotechnology, Bharathidasan University, Tiruchirappalli, TN-620 024, India.

* Corresponding author e-mail: achiramans@bdu.ac.in

Abstract

The silver nanoparticles (Ag NPs) were derived from *Acorus calamus* (*A. calamus*) rhizome extract using different temperature. The absorbance centered at 439 nm, which was corresponds to the wavelength of the surface plasmon resonance of Ag NPs at 95 ◦C. From FESEM and TEM image showed, the Ag NPs were exhibited spherical structure. Elemental compositions were identified by EDAX analysis. The synthesized Ag NPs, functional groups were identified by the FTIR spectra. The antibacterial studies performed against a set of bacterial strains showed that the Ag NPs possessed a greater antibacterial effect than the Plant extract (PE) and silver nitrate. *In-vitro* cytotoxic effect of green synthesized *A. calamus* rhizome extract derived Ag NPs tested against MG 63, MCF-7 and HeLa cell lines.

Keywords: Silver NPs, *A. calamus* rhizome extract, green synthesis, anticancer activity.

Introduction

Silver nanoparticles (Ag NPs) are interesting field of active research based on their unique feature such as optical and electrical properties [1,2] and its extensive application in various areas such as antimicrobial [3], anticancer [4] and catalysis [5]. Based on the size and shape nanoparticles have been prepared by various methods such as chemical method physical method [6] and Green method [7]. Among this methods Green synthesis is offers a comparatively safer and eco-friendly approach for nanoparticle synthesis. Green synthesis processes are ahead much attention as a possible alternative for the development of Metal and metal-oxide nanoparticles, where natural plant materials are used without any chemical reducing reagent.

Acorus calamus (*A. calamus*) belongs to the order Acorales and family Acoraceae. It has numerous medicinal aids. Rhizome is used to treat gastrointestinal problems that include inflammation of stomach, flatulence, ulcers and anorexia and other medicinal uses of *A. calamus* are induction of sweating, treatment of stroke and treatment of rheumatoid arthritis. The *A. calamus* is used as sedative in form of calming medicine. However, this plant acts as stimulant and also as hallucinogen, which is commonly used to treat skin diseases and is broadly used as spices [8]. The synthesis of Ag NPs from natural plant extract is considered to be the most suitable method on the ecological problems.

In present work, silver NPs are derived *Acorus calamus* extract using green approach. We have studied the structural, optical, antibacterial and anticancer properties of Ag NPs. To the best of our knowledge, this is the first report on the bio-synthesis of silver NPs by using *Acorus calamus* rhizome extract and their

characterization studies such as UV-Visible, FESEM, TEM, EDAX FT-IR, DLS, Zeta potential, antibacterial and anticancer activity were carried out.

Material and methods

Collection of plant Materials

A. calamus is important aromatic plant which mainly found in wet and marshy places. The natured rhizome of *Acorus calamus* was collected from well-grown plants in kollimalai hills, Namakal, Tamilnadu, India. The plant materials were identified by the department of plant science, Bharathidasan University, Tiruchirappalli collected from kollimalai hills. The plant materials were picked and washed with double distilled water to remove dust particles and shade dried for 40 days at 25±5 ºC. The dried plant materials were grind to the finest powder form and % aqueous *Acorus Calamus* rhizome extract was prepared with Millipore water and incubated at 60 ºC for 10 minutes and used for the bio-reduction.

Preparation of Silver Hydrosol:

The preparation of the nanoparticles was following protocols used by song and kim [9]. 5ml of the hydrosol was added to 95ml of 1mM aqueous silver nitrate (Qualigens-99.8%) solution. The silver nitrate solution mixture was slowly heated in a water bath at varying temperature range from 30ºC to 95ºC. To confirm that better separation from free entities, the brown hydrosol was centrifuged at 10,000 rpm for 20 minutes at 4ºC and repeated three times to remove undispersed residues.

Evaluation of antimicrobial activity

The bacterial strains *Klebsiella pneumonia (ATCC 13883)*, *Pseudomonas aeruginosa* (ATCC 27853), *Citrobacter diversus* (ATCC 27156) and *Escherichia coli* (ATCC 25922) were obtained from ATCC, American of Microbial Technology (IMTECH), Chandigarh, India and used for analysis of bactericidal activities.

A disk diffusion method was adopted to assay the NPs for bactericidal activity against the test strains on Luria Bertani (LB) agar plates. This Ag NPs were performed by determining the Zone of inhibition and which was rapid and inexpensive to determine the susceptibility of a particular antigen to the bactericidal agent applied [10]. This was executed by measuring the diameter (mm) of the area that stays clear of microbial growth using a Vernier caliper. To accomplish this method, standard antibiotic disks were purchased from HIMEDIA Laboratories, India. Each disk had a diameter of 6 mm and was loaded with 25 µL of the test sample and air dried. Bacterial cultures about 10^6 CFU/mL were spread plated on LB agar, impregnated with the sample loaded disks and incubated at 37 ◦C for 24 h. The diameters of Zone of inhibition were measured and the assays were performed in triplicate.

Cell culture

In vitro tissue culture experiments were carried out with human breast cancer cell line (MCF7), Human cervical cancer cell line (HeLa) and Human osteosarcoma cell lines (MG 63) which were obtained from National Centre for Cell Science (NCCS). These cell lines were propagated in Eagles Minimum Essential Medium (EMEM), supplemented with 10% fetal bovine serum (Sigma, USA) and 10,000 IU penicillin and 100 µg/ml of streptomycin as antibiotics (Himedia, Mumbai, India), in 96 well culture plates, at 37 ˚C, in a humidified atmosphere of 5% CO_2, in a CO_2 incubator. All experiments were performed using cells from passage 15 or less.

Cell treatment procedure

The monolayer cells were detached with trypsin-ethylene diamine tetra acetic acid (EDTA) to make single cell suspensions. The viable cells were counted by tryphan blue exclusion assay using a hemocytometer.

The cell suspension was diluted with medium containing 5% FBS to give final density of $1x10^5$ cells/ml and 100 µl per well of cell suspension were seeded into 96-well plates at plating density of 10,000 cells/well and incubated to allow for cell attachment at and 100% relative humidity. After 24 h the cells were treated with different concentrations of the test 37 ◦C, 5% CO_2, 95% air samples. The samples were initially dissolved in DMSO and diluted to twice the desired testing final concentration with serum free medium. Additional four, serial dilutions were made to provide a total of five sample concentrations. Aliquots of 100 µl of these different sample dilutions were added to the appropriate wells already containing 100 µl of medium, resulted the required final sample concentrations. Following drug addiction the plates were incubated for an additional 48 h at 37 ◦C, 5% CO_2, 95% air and 100% relative humidity. The medium containing without samples were served as control and triplicate was maintained for all concentrations.

MTT assay

The biosynthesis Ag NPs were suspended in dimethyl sulfoxide (DMSO), diluted in culture medium and used to treat the chosen cell lines MCF-7, HeLa and MG 63 over a complex concentration range of 3.125-50 µl/ml for 24 h and 48 h. DMSO solution was used as the solvent control.

A miniaturized viability assay using 3- (4, 5-di-methylthiazol-2-yl)-2, 5-diphenyl-2H-tetrazolium bromide (MTT) was carried out. To each well, 20 µl of 5 mg/ml MTT in phosphate buffer (PBS) was added. The plates were wrapped with aluminum foil and incubated for 4 h at 37 ˚C. The purple formazan product was dissolved by the addition of 100 µl of 100% DMSO to each well. The absorbance was monitored at 570 nm (measurement) and 630 nm (reference) using a 96 well plate reader (BioRad, Hercules, CA, USA).

The data were collected for four replicates. The percentage of inhibition was calculated from this data using the formula

$$\frac{mean\ OD\ of\ untreated\ cells\ (control) - mean\ OD\ of\ treated\ cells}{mean\ OD\ of untreated\ cells\ (control)} \text{ x } 100$$

Cytotoxic assay (ex-vivo)

Tumor cell lines and determination of cell viability

Dalton lymphoma asciteaes (DLA) cells were obtained as a generous gift from Amala Cancer Research Center, Thrisur, and Kerela, India. They were maintained by weekly intra-peritoneal inoculation of 10^6 cell/ per mouse.

Determination of tumor cell count

The tumor fluid was taken in a RBC pipette and diluted 1000 times. Then a drop of the diluted cell suspension was placed on the Neubauer counting chamber and the number of cells in 64 small squares was counted [11]. The cell were then stained with trypan blue (0.4% in normal saline) dye. The cells that did not take up the dye were viable and those that took the stain were nonviable. These viable and nonviable cells were counted.

Cell count = (No. of cells x Dilution) / (Area x Thickness of liquid film).

Results and discussion

The *A. calamus* rhizome extract was used to synthesis for Ag NPs. The during synthesis, plant extract with Ag NPs color change to brown were visually observed for all the hydrosols at 30 ˚C, 60 ˚C, 90 ˚C and 95 ˚C with the hydrosol at 90 ˚C and 95 ˚C with formation of yellowish brown color (Fig. 1). Figure 2 shows the UV-Vis absorption spectra of synthesized Ag NPs with different temperature. The absorption peaks are obtained at 315 nm, 415 nm, 432 nm, 423 nm and 439 nm for PE, 30 ˚C, 60 ˚C, 90 ˚C and 95 ˚ for Ag NPs respectively. The UV-Vis absorption peak ranges between 410-450 nm are attributes to the Surface Plasmon Resonance (SPR) of Ag NPs in particles sizes range of 25-50 nm [12, 13]. From the literature, the SPR in the region of around 410-450 nm can be attributed to spherical nanoparticles [14, 15].

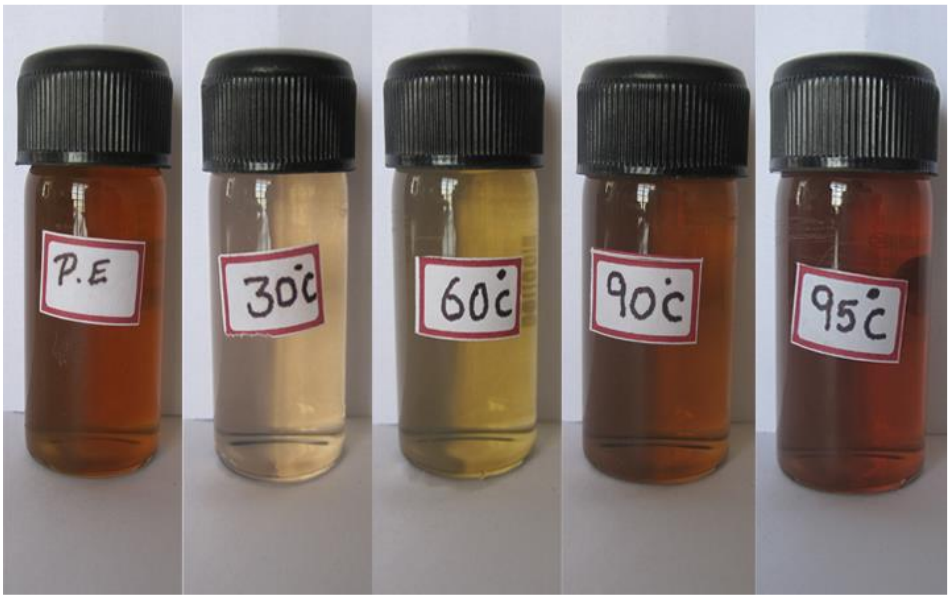

Figure 1 Colour change profile of Ag NPs derived *A. calamus* rhizome extract at different temperature.

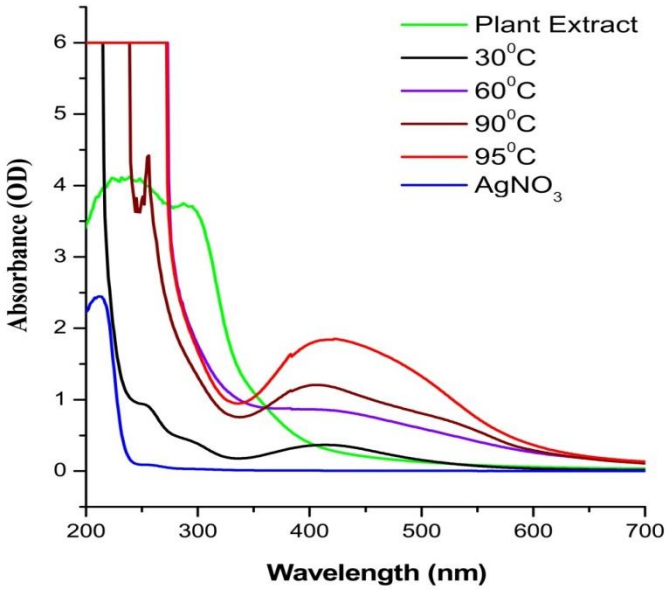

Figure 2 Uv-Vis absorbance spectra of Ag NPs derived *A. calamus* rhizome extract.

Vibrational spectra of the synthesized Ag NPs are shown in Fig. 3. In literature, O-H stretching frequencies at 3439 cm^{-1} and 1630 cm^{-1} [16]. From the FTIR result, broad O-H stretching frequencies are observed at 3432 cm^{-1} and 1637 cm^{-1} for Ag NPs. The week C ≡ N nitrile group is center at 2394 cm^{-1}. The C-OH bending vibration is observed at 1485 cm^{-1} for Ag NPs. The broad absorption peak at 688 cm^{-1} can be due to the O-H bends related to phenolic constituents of the plant [17].

The morphology of the Ag NPs synthesized by *A. calamus* is shown in Fig. 4(a-b). The entire FESEM and TEM image, the silver NPs are exhibited spherical structure. The average particles size range between 30-50 nm.

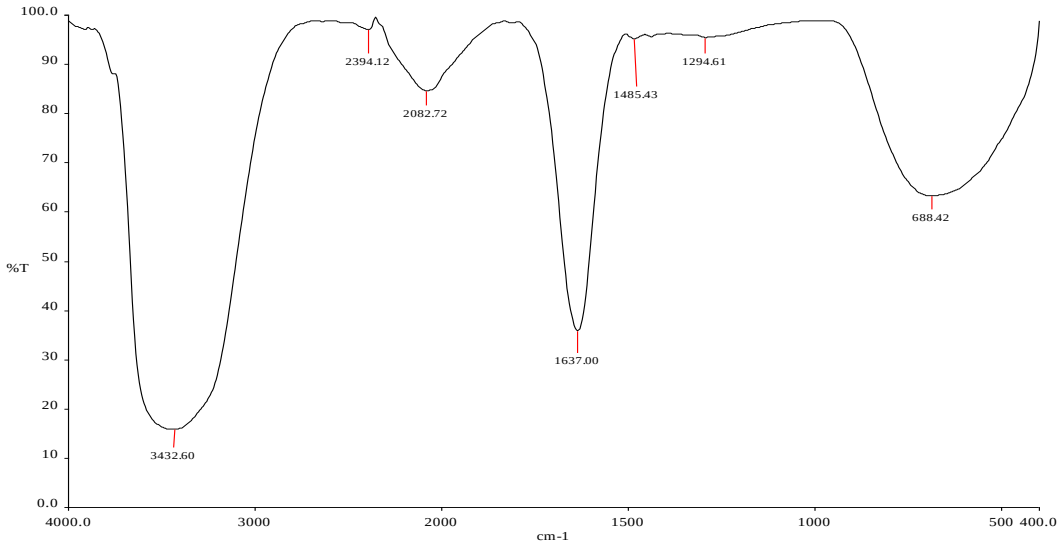

Figure 3 FT-IR analysis of Ag NPs derived *A. calamus* rhizome extract.

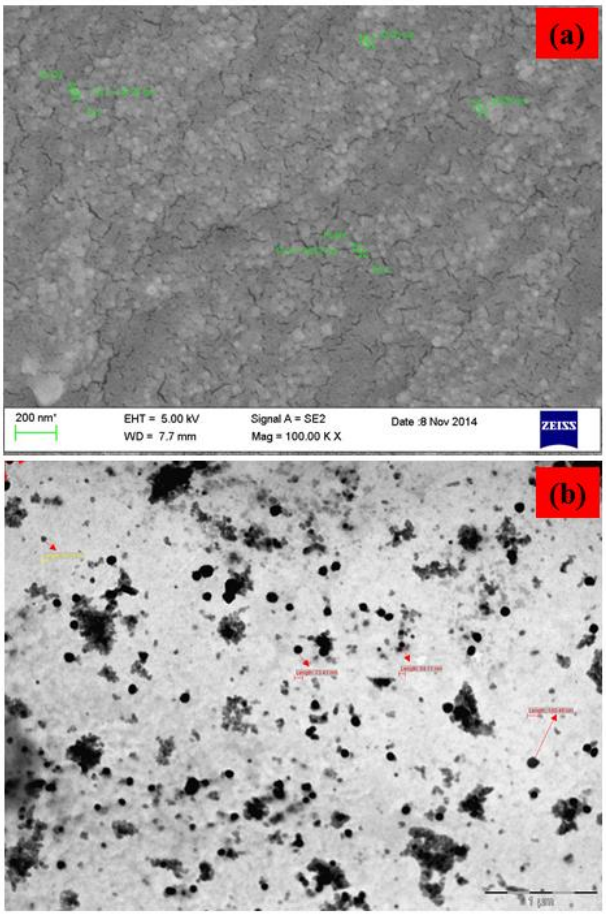

Figure 4(a-b) FESEM and TEM image of Ag NPs derived *A. calamus* rhizome extract.

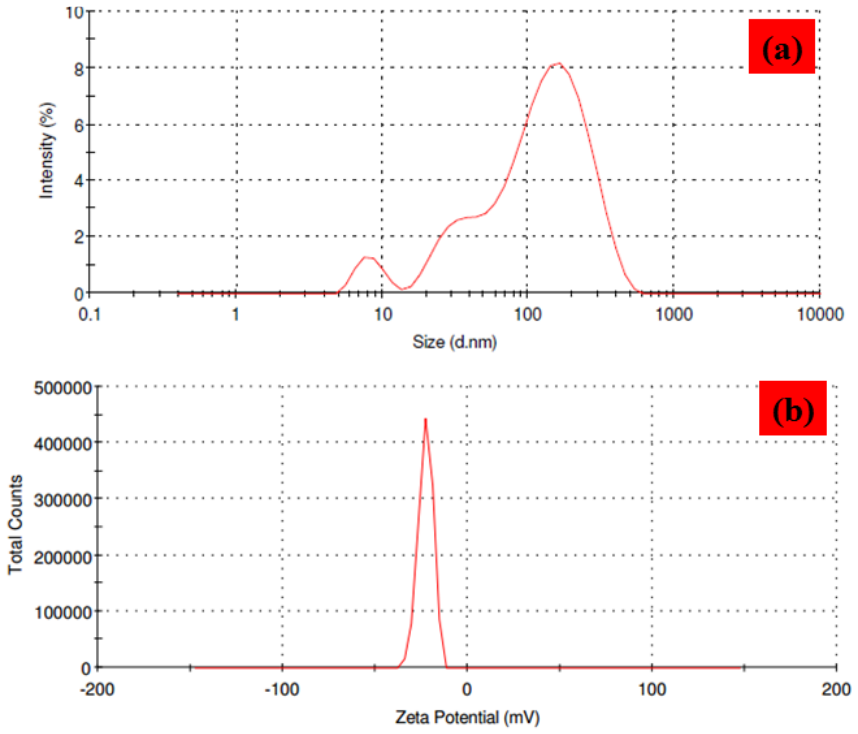

Figure 5 DLS and Zeta potential analysis of the Ag NPs derived *A. calamus* rhizome extract.

Zeta potential analysis revealed the surface charge of found to be -22.6 mV indicating highly stable Ag NPs are shown in Fig. 5. Potential of the Ag NPs sample move towards the vicinity of zero, the particles tend to aggregate. Negative charge of particles has a tendency to high stability of particles from agglomeration leading to stable nanoparticles [17].The average particle size 72.89 nm for Ag NPs measured by dynamic light scattering is shown in Fig. 2B. Dynamic light scattering being a sensitive for detection of plant molecules bound nanoparticles can detect smaller amounts of large sized particles formation due to agglomeration disturbing in particle sizes [18].

The elemental composition used to identify by EDAX spectra of the biosynthesis of Ag NPs is shown Fig. 6. The Ag metal contents are found to be major weight 82.20%. Which was due to the traces of bio-capping materials may be on the surface of Ag NPs. These bio-capping materials influence of the responsible for the reduction as well as stabilization of Ag NPs and also traces of C (5.95%) and O (11.85%) observed for Ag NPs values are given in Table 1.

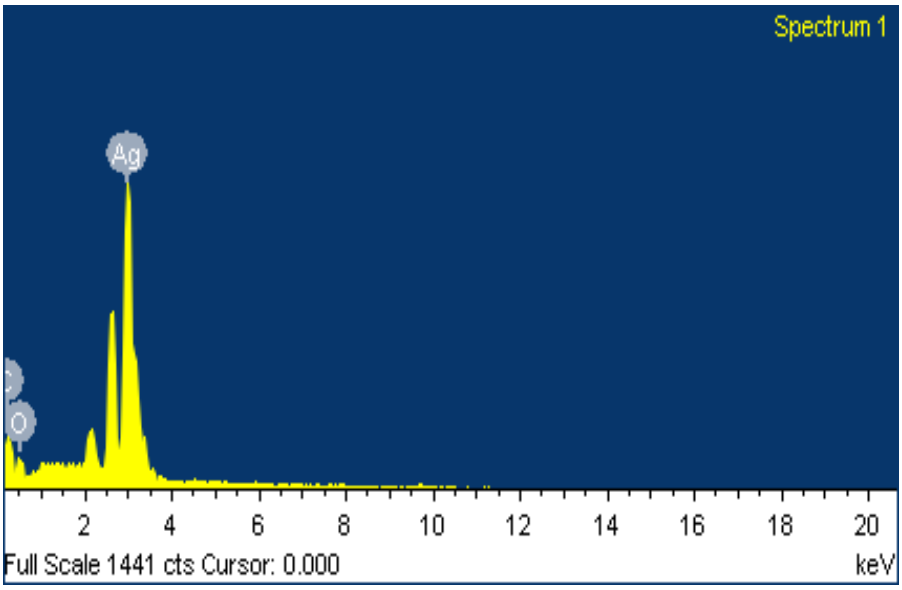

Figure 6 EDAX spectra of the Ag NPs derived *A. calamus* rhizome extract.

Element	**Weight %**
C	**5.95**
O	**11.85**
Ag	**82.20**
Totals	**100.00**

Table 1 Elemental composition of Ag NPs.

In present work, Ag NPs derived *A. calamus* rhizome extract is tested against *K. pneumonia*, *P. aeruginosa*, *C. diversus* and *E.coli* studied disc diffusion method are shown in Fig. 7. Table 2 shows the zone of inhibition of PE, silver nitrate salt and Ag NPs are treated with respective bacterial strains. From the table 2 showed the Ag NPs are possessing more antibacterial activity as compared to that plant extract and silver nitrate salt.

The silver NPs are large surface area, which provides improved contact with microorganisms. The nanoparticles are attached to the cell membrane and also penetrate inside the bacteria. The bacterial membrane contains sulfur-containing proteins and the silver NPs interact with protein cell wall and the phosphorus containing compounds like DNA. The Ag NPs enter the bacterial cell it forms a low molecular weight region in the center of the bacteria to which the bacteria conglomerates thus, protecting the DNA from the silver ions. The nanoparticles preferably attack the respiratory chain, cell division finally leading to cell death. The nanoparticles release Ag^+ ions in the bacterial cells, which enhance their bactericidal activity [19]. The size of the nanoparticle implies that it has a large surface area to come in contact with the bacterial cells hence; it will have a higher percentage of interaction than bigger particles [19]. In FESEM and TEM image result, Ag NPs average size less than 30-50 nm interact with bacteria and produce electronic effects, which enhance the reactivity of nanoparticles. It is verified that the bactericidal effect of Ag NPs are size dependent [19].

The Ag NPs exhibited relative superior activity against all the pathogens, its minimum inhibitory concentration (MIC) is determined. The MIC results for all of the test pathogens are summarized in Table 3. The minimum concentration of Ag NPs required inhibiting the growth of *K. pneumonia*, *P. aeruginosa*, *C. diversus* and *E.coli* are 62.5μg/ml, 31.25 μg/ml, 62.5 μg/ml and 31.25 μg/ml which suggested that the Ag NPs exhibit better antibacterial activity than the plant extract and silver nitrate salt.

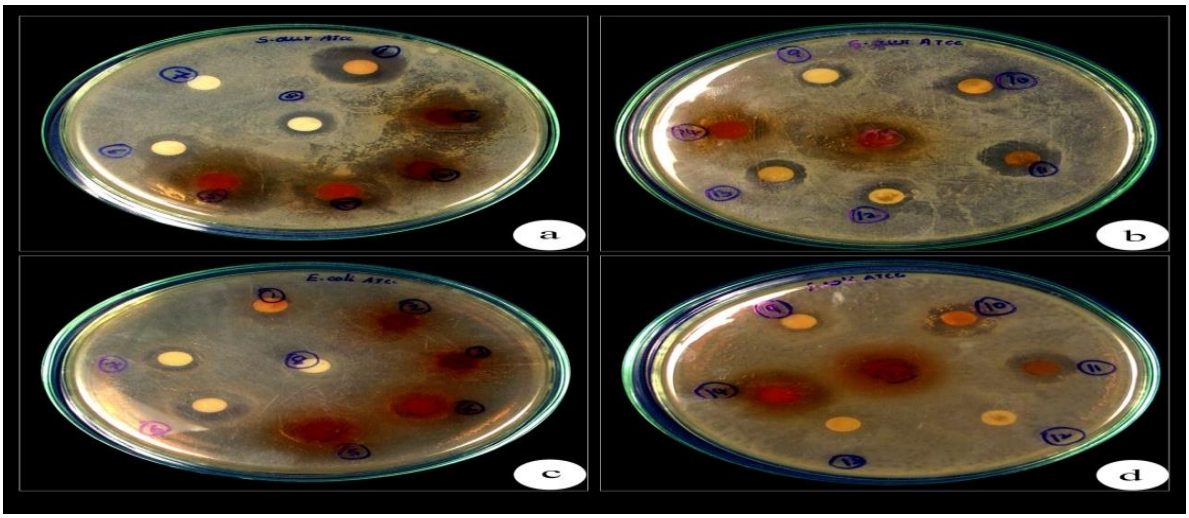

Figure 7 Zones of Inhibition (mm) of Ag NPs derived *A. calamus* rhizome extract, Plant extract alone (1%) and Silver nitrate (1mM) against a few standard ATCC bacteria (a) *K. pneumonia*, (b) *P. aeruginosa*, (c) *C. diversus* and (d) *E.coli*.

Bacteria	**Zones of inhibition in (mm)**		
	PE	**$AgNO_3$**	**Ag NPs**
K. pneumonia ATCC 13883	12	7	15
P. aeruginosa ATCC27853	11	6	17
C. diversus ATCC 27156	12	9	19
E.coli ATCC25922	11	8	16

Table 2 Mean Zones of Inhibition (mm) of the silver nanoparticles synthesized using aqueous extract of *A. calamus* (1%), Plant extract alone (1%) and Silver nitrate (1mM) against a few standard ATCC bacteria.

Bacteria	**MIC (μg/ml)**		
	PE	**$AgNO_3$**	**Ag NPs**
K. pneumonia ATCC 13883	250	500	62.5
P. aeruginosa ATCC27853	250	500	31.25
C. diversus ATCC 27156	500	125	62.5
E. coli ATCC 25922	62.5	250	31.25

Table 3 Minimal inhibitory concentrations (μg/ml) of the Ag NPs derived *A. calamus* rhizome extract (1%), Plant extract alone (1%) and Silver nitrate (1mM) against a few standard ATCC bacteria.

The cytotoxic effect of Ag NPs were examined in cultured (MG-63) human osteosarcoma cancer, (MCF-7) human breast cancer and (HeLa) cervical cancer cell lines (see Fig. 8-10) by exposing cells for 24 h to culture medium containing the Ag NPs at 15.52 μl/mL, 13.96 μl/mL and 10 μl/mL for IC_{50} concentration is given in Table 3-5. In relation to (HeLa) cervical cancer cell death, a minimum concentration 10 μl/mL for 24 h treatment of Ag NPs was well enough to induce 50% cell mortality. The cytotoxic efficiency of the Ag NPs generally depends on the presence of Reactive oxygen species (ROS), which is mainly attributed small size of the nanoparticles. This is causing to the generation of more hydrogen peroxide (H_2O_2). Apoptosis has been implicated as a major mechanism of cell death caused by nanoparticle induced oxidative stress [20]. Among the different apoptotic pathways, the intrinsic mitochondrial apoptotic pathway plays a major role in metal oxide nanoparticle-induced cell death, since mitochondria are one of the major target organelles for nanoparticle-induced oxidative stress [21]. The high levels of ROS in the mitochondria can result in damage to membrane phospholipids inducing mitochondrial membrane depolarization [22]. The small proportion of electrons escapes from the mitochondrial chain and interacts with molecular oxygen to form $\cdot O_2^-$ which later gives rise to H_2O_2. The nanoparticle can catalyze the $\cdot O_2^-$ generation either by blocking the electron transport chain or accelerating electron transfer to molecular oxygen [23]**.**

Concentration (µl/ml)	**% Cell Inhibition**
3.125	**0.405093**
6.25	**0.636574**
12.5	**6.018519**
25	**99.76852**
50	**100**

Table 3 *In vitro* cytotoxicity of the Ag NPs derived *A. calamus* rhizome extract against MG 63-cell line.

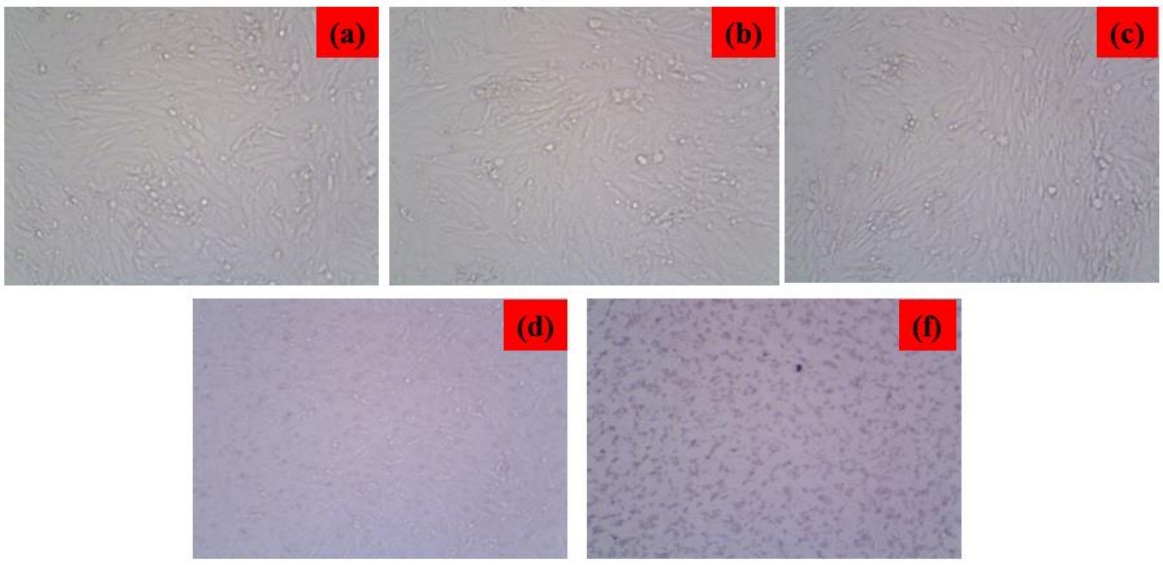

Figure 8 *In vitro* cytotoxicity of the Ag NPs derived *A. calamus* rhizome extract against MG 63-cell line.

Concentration (µl/ml)	**% Cell Inhibition**
3.125	**0.361272**
6.25	**0.794798**
12.5	**29.91329**
25	**98.98844**
50	**100**

Table 4 *In vitro* cytotoxicity of *A. calamus* derived Ag NPs against MCF-7 cell line.

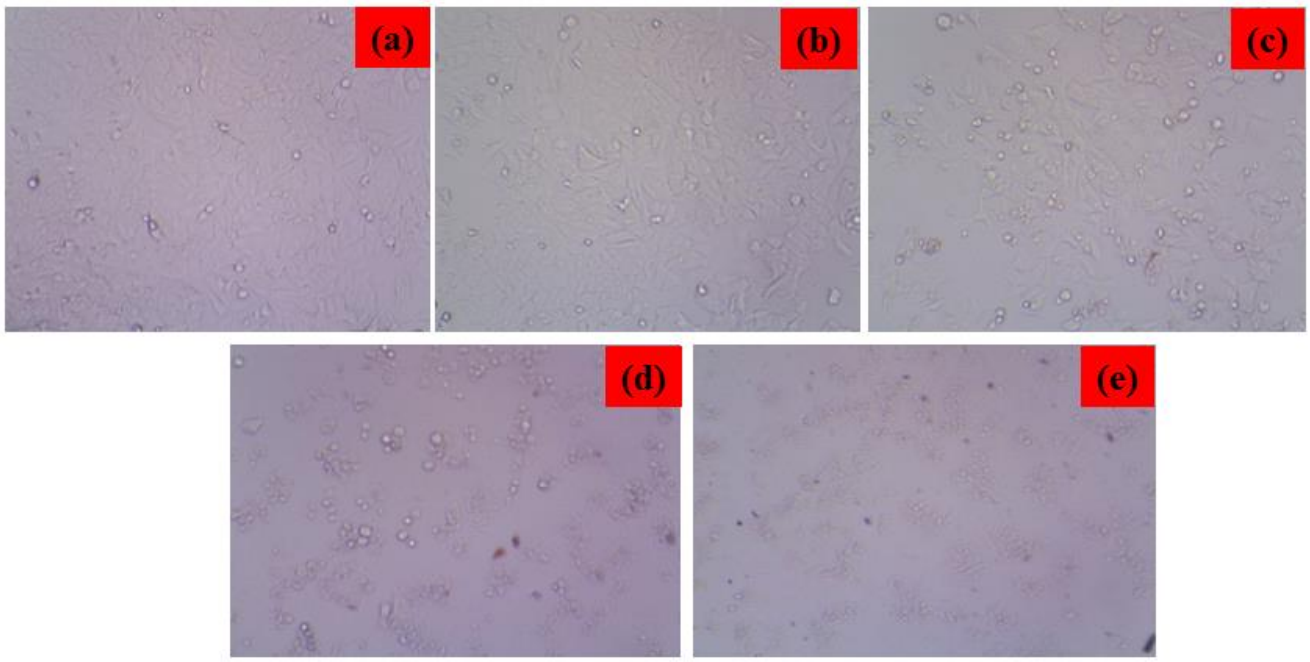

Figure 9 *In vitro* cytotoxicity Ag NPs derived *A. calamus* rhizome extract against MCF 7- cell line.

Concentration (µl/ml)	**% Cell Inhibition**
0.01	**-0.70243**
0.1	**2.873563**
1	**5.491699**
5	**7.535121**
50	**100**

Table 5 *In vitro* cytotoxicity of the Ag NPs derived *A. calamus* rhizome extract against HeLa-cell line.

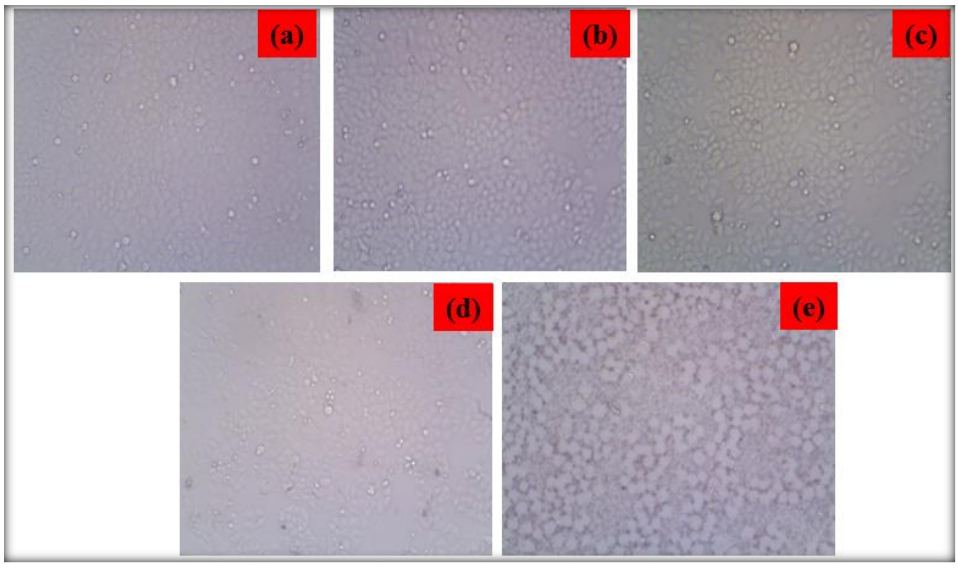

Figure 10 In vitro cytotoxicity of the Ag NPs derived *A. calamus* rhizome extract against HeLa-cell line

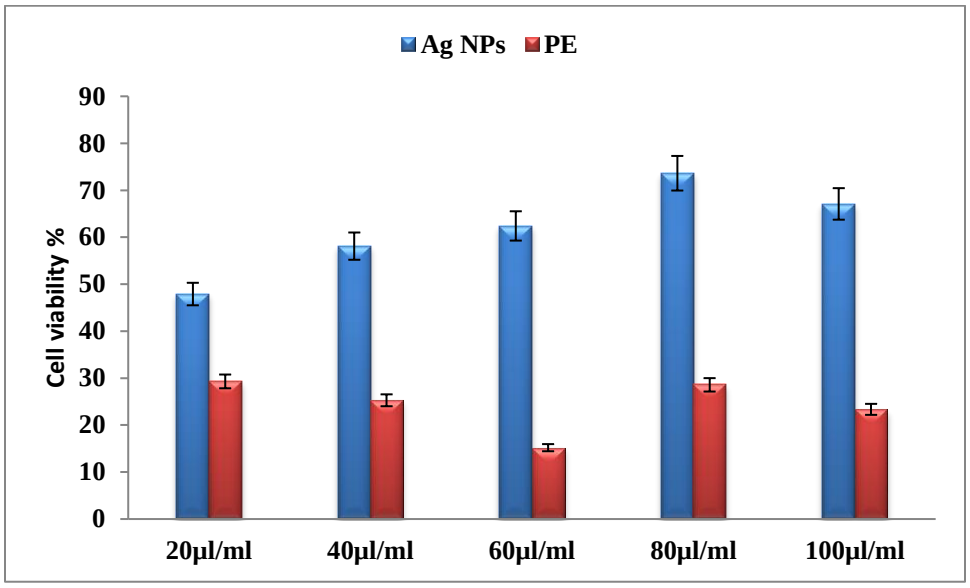

Figure 11 Effect of the Ag NPs derived *A. calamus* rhizome extract on tumor cells ex vivo.

Nanoparticles have the potential to improve cancer therapy [20]. The cytotoxicity of green synthesized Ag NPs and Plant extract treated again DAL cells were confirmed by ex vivo studies. A series of different doses such as 20 µl/ml, 40 µl/ml, 60 µl/ml, 80 µl/ml and 100 µl/ml are used and the IC_{50} concentration was found to be approximately 40 µl/ml for Ag NPs are shown in Fig 11.

Conclusions

In summary, *A. calamus* rhizome extract derived Ag NPs were confirmed at 95°C with formation of yellowish brown color. These color change appearance arise due to the excitation of surface plasmon resonance in synthesized nanoparticles. From the UV-Vis result, the absorbance centered at 439 nm, which was corresponds to the wavelength of the surface plasmon resonance of Ag NPs at 95 ◦C. FESEM and TEM images, the Ag NPs were exhibited spherical structure and

average particles size 30-50 nm. Elemental compositions were used identified by EDAX spectra. From DLS measurement, the size distribution at 72.89nm for *A. calamus* rhizome extract derived Ag NPs. Zeta potential analysis, the stability of Ag NPs was observed at - 22.6 meV. The organics functional groups were identified by FTIR spectra. The ***A. calamus*** rhizome extract derived Ag NPs, PE and silver nitrate were tested again *K. pneumonia*, *P. aeruginosa*, *C. diversus* and *E.coli* strain, Ag NPs possesses more antibacterial activity as compared to that PE and silver nitrate. *In-vitro* cytotoxic effect of green synthesized *A. calamus* rhizome extract derived Ag NPs tested against HeLa, MCF-7 and MG 63 cell lines. *A. calamus* rhizome extract derived Ag NPs were potential anticancer agent for cytotoxic effect to cancerous cells. *Ex-vivo* studies revealed the cytotoxic concentration of Ag NPs against DLA cells.

References

[1] Mahmudin, L., Suharyadi, E., Utomo, A. B. S., & Abraha, K. (2015). Optical properties of silver nanoparticles for surface plasmon resonance (SPR)-based biosensor applications. J. Mod. Phys., 6 1071-1076.

[2] Chen, D., Qiao, X., Qiu, X., & Chen, J. (2009). Synthesis and electrical properties of uniform silver nanoparticles for electronic applications. Journal of Materials Science, 44(4), 1076-1081.

[3] Ali, M. R., Umaralikhan, L., & Jaffar, M. (2015). Antibacterial Effect of Silver Nanoparticles Synthesized Using Curcuma Aromatica Leaf Extract.

[4] Majeed, S., bin Abdullah, M. S., Nanda, A., & Ansari, M. T. (2016). In vitro study of the antibacterial and anticancer activities of silver nanoparticles synthesized from Penicillium brevicompactum (MTCC-1999). Journal of Taibah University for Science, 10(4), 614-620.

[5] Santos, K. D. O., Elias, W. C., Signori, A. M., Giacomelli, F. C., Yang, H., & Domingos, J. B. (2012). Synthesis and catalytic properties of silver nanoparticle–linear polyethylene imine colloidal systems. The Journal of Physical Chemistry C, 116(7), 4594-4604.

[6] Iravani, S., Korbekandi, H., Mirmohammadi, S. V., & Zolfaghari, B. (2014). Synthesis of silver nanoparticles: chemical, physical and biological methods. Research in pharmaceutical sciences, 9(6), 385-406.

[7] Umaralikhan, L., & Jaffar, M. J. M. Green Synthesis of MgO Nanoparticles and it Antibacterial Activity. Iranian Journal of Science and Technology, Transactions A: Science, 1-9.

[8] Ganesan, R. M., & Prabu, H. G. (2015). Synthesis of gold nanoparticles using herbal Acorus calamus rhizome extract and coating on cotton fabric for antibacterial and UV blocking applications. Arabian Journal of Chemistry.

[9] Song, J. Y., & Kim, B. S. (2009). Rapid biological synthesis of silver nanoparticles using plant leaf extracts. *Bioprocess and biosystems engineering*, *32*(1), 79-84.

[10] Yu, D. G. (2007). Formation of colloidal silver nanoparticles stabilized by Na+–poly (γ-glutamic acid)–silver nitrate complex via chemical reduction process. *Colloids and Surfaces B: Biointerfaces*, *59*(2), 171-178.

[11] Gupta, M., Mazumder, U. K., & Gomathi, P. (2007). In vitro antioxidant and free radical scavenging activities of Galega purpurea root. *Pharmacognosy Magazine*, *3*(12), 218.

[12] Sivalingam, P., Antony, J. J., Siva, D., Achiraman, S., & Anbarasu, K. (2012). Mangrove Streptomyces sp. BDUKAS10 as nanofactory for fabrication of bactericidal silver nanoparticles. *Colloids and Surfaces B: Biointerfaces*, *98*, 12-17.

[13] Panáček, A., Kvítek, L., Prucek, R., Kolář, M., Večeřová, R., Pizúrová, N., Sharma, V.K., Nevěčná, T.J. and Zbořil, R., 2006. Silver colloid nanoparticles: synthesis, characterization, and their antibacterial activity. *The Journal of Physical Chemistry B*, *110*(33), pp.16248-16253.

[14] Mock, J. J., Barbic, M., Smith, D. R., Schultz, D. A., & Schultz, S. (2002). Shape effects in plasmon resonance of individual colloidal silver nanoparticles. *The Journal of Chemical Physics*, *116*(15), 6755-6759.

[15] Zaheer, Z. (2012). Silver nanoparticles to self-assembled films: green synthesis and characterization. Colloids and Surfaces B: Biointerfaces, 90, 48-52.

[16] Shivakumar, M., Nagashree, K. L., Yallappa, S., Manjappa, S., Manjunath, K. S., & Dharmaprakash, M. S. Biosynthesis of silver nanoparticles using pre-hydrolysis liquor of Eucalyptus wood and its effective antimicrobial activity. *Enzyme and Microbial Technology*, (2017) *97*, 55-62.

[17] U. Suriyakalaa, J. J. Antony, S. Suganya, D. Siva, R. Sukirtha, S. Kamalakkannan, P. B. U Suriyakalaa, U., Antony, J. J., Suganya, S., Siva, D., Sukirtha, R., Kamalakkannan, S., ... & Achiraman, S. (2013). Hepatocurative activity of biosynthesized silver nanoparticles fabricated using Andrographis paniculata. *Colloids and Surfaces B: Biointerfaces*, *102*, 189-194.

[18] S. A. Cumberland, J. R. Lead, J. R. (2009). Particle size distributions of silver nanoparticles at environmentally relevant conditions. *Journal of chromatography A*, *1216*(52), 9099-9105.

[19] M. Rai, A. Yadav, A. Gade, (2009). Silver nanoparticles as a new generation of antimicrobials. *Biotechnology advances*, *27*(1), 76-83.

[20] J. Boonstra, J. A. Post, (2004) Molecular events associated with reactive oxygen species and cell cycle progression in mammalian cells, Gene, , 337, 1-13.

[21] M. M. Wang, Y. C. Wang, X. N. Wang, Y. Liu, H. Zhang, J. W. Zhang, Q. Huang, P. S. Chen, K. T. Hei, L. J. Wu, A. Xu, (2015) Mutagenicity of ZnO nanoparticles in mammalian cells: Role of physicochemical transformations under the aging process. Nanotoxicology, 13, 1-11.

[22] Y. Shi, F. Wang, J. He, S. Yadav, H. Wang, (2010) Titanium dioxide nanoparticles cause apoptosis in BEAS-2B cells through the caspase 8/t-Bid-independent mitochondrial pathway, Toxicol. Lett., 196, 21-27.

[23] P. Manna, M. Ghosh, J. Ghosh, J., Das, P. C. Sil, (2012) Contribution of nano-copper particles to *in vivo* liver dysfunction and cellular damage: Role of I*κ*B*α*/NF-*κ*B, MAPKs and mitochondrial signal, Nanotoxicology, 6, 1-21.

[24] D. Peer, J. M. Karp, S. Hong, O. C, Farokhzad, R. Margalit, & R. Langer, (2007). Nano carriers as an emerging platform for cancer therapy. *Nature anotechnology*, *2*(12), 751-760.